Iterative robust numerical procedure for the determination of kinetic constants in Han's model for NR cured with sulphur

G. Milani[1] · **F. Milani**[2]

Received: 5 October 2014 / Accepted: 17 March 2015 / Published online: 28 March 2015

✉ G. Milani
milani@stru.polimi.it; gabriele.milani@polimi.it

1 Politecnico di Milano, Piazza Leonardo da Vinci 32, 20133 Milan, Italy

2 Chem.Co Consultant, Via J.F.Kennedy 2, 45030 Occhiobello, RO, Italy

1 Introduction

The vulcanization with sulphur of natural rubber (NR) dates back to the second half of nineteenth century. Unfortunately it is particularly complex, involves long polymer chains with single and multiple transversal sulphur bonds, it exhibits deterioration of the mechanical properties after long curing at high temperatures (reversion), it is pro-moted when a number of accelerators and coadiuvants are added to the blend, improves considerably when loaded with carbon black, all the ingredients mixed together in variable concentrations, almost always not known by the providers. For these reason, despite the immediate success and its widespread diffusions in practical applications within automotive industry, tires and many other fields, its chemistry of reaction is still for some extent not fully clear [1,2]. As a consequence, it remains difficult to propose efficient numerical tools aimed at predicting the vulcanization degree of a given rubber item, in relation, also, to the typology of rubber investigated.

The traditional and cheapest experimental test used within the rubber industry to have an insight into the degree of vulcanization of a blend during thermal curing is certainly the rheometer test [3]. A rheometer is a device where a rubber sample of few grams is cured at constant temperature. In traditional rheometers, a disc present inside the vulcanization chamber, oscillates regularly with small angles (typically 3 °). The resistance to oscillation is measured with the torque applied to the disc. The resultant time–torque curve is the fingerprint of the blend, varying considerably from blend to blend and for the same blend at different temperatures. Some features are however common to all samples: torque generally starts to increase very slowly (or decreases) during a so called "induction" period, after which curing starts to take place quite fast, with an increase of the crosslink density and hence of the measured macroscopic torque. Very frequently, NR exhibits also marked reversion, a phenomenon that usually is more visible at high temperatures and that consists into a decrease of the measured torque. Typically reversion is attributed to the formation and subsequent degradation of poly-sulphidic (S–S or more) crosslinks [4–7], which are thermodynamically less stable than mono-sulphidic links [7].

There is experimental evidence of polysulfidic structures obtained with costly IR, UV, ESR and Raman characterizations [8,9] or with chemical methods [10], as well as solid state ^{13}C nuclear magnetic resonances (NMRs) [11–13]. It has been shown that for EPDM, the polysulfidic structures are consistent with predictions based on model compounds and the presence of three different allylic positions in the repeating unit of NR [11]. The percentage of each polysulfidic structure and the number of concatenated sulphur depend on both rubber structure and curing temperature and time of exposition [14]. It is also interesting to point out that experimentation shows

that, at the beginning of vulcanization, more $C-S_x-C$ ($x = 4, 5$ or more) bonds are present. It is intuitively assumed that ($C-S_x-C$) polysulfidic crosslinks further react, leading either to shorter crosslinks (C–S–C and C–S–S–C), through a so called "maturation reaction", or to cyclic polysulfidic structures (backbiting). By means of maturation, crosslinking density decreases, and this explains from a chemical point of view the macroscopically observed reversion.

As well-known from decades, reversion phenomenon is linked to temperature: high curing temperatures are always associated to fast vulcanization with torque drops immediately after maximum point; conversely, at low temperatures rheometer curves exhibit no reversion with low curing rates. It is interesting to point out that very recently, Leroy et al. [15] and Milani et al. [16–18] have shown numerically that the ratio between thermally stable (short) and unstable (long) polysulfidic crosslinks seems not significantly influenced by cure temperature, instead they seem strictly related to the typology of accelerators used, and hence to the chemical nature of the activated complexes inside the blend.

There are several models in the literature that allow a fair prediction of the curing percentage of NR vulcanized into a rhoemeter. Most of them are mechanistic, as those by of Coran [6], Ding and Leonov [19,20], Kamal and Sorour [21] or a semi-mechanistic (model of Han et al. [1], Loroy et al. [15], Milani et al. [2,18]).

The majority of such approaches is based on a preliminary presentation of the kinetic scheme describing in an approximate way NR sulphur curing. Such scheme is obviously a simplification of the real one and comes from the translation of macroscopic observations (e.g. induction, primary curing, stabilization and reversion) into chemical reactions. From classic kinetic theory, the set of chemical reactions is again translated into mathematics, namely a system of partial differential equations (PDEs).

To provide a rheometer curve, the system of differential equations must be solved numerically through a Runge-Kutta approach. This is certainly a drawback, also in light of the fact that practitioners active in this field are not always familiar with classic but non trivial numerical procedures like those necessary to deal with PDEs, or simply they do not dispose of licensed dedicated software. The second important limitation is that an estimate of such kinetic constants should be done minimizing the total error of the numerical curve on the normalized experimental one. Least-squares fitting is the most popular approach. In practice, the combination of PDEs and least-squares means the iterative solution of several PDEs, until a converged solution is found by least-squares. Unfortunately, for the problem at hand, it is possible to find sub-optimal solutions where the experimental rheometer curve fitting is satisfactory but the estimation of the kinetic constants is totally unrealistic. This is rather common in presence of non linear problems with multiple local minimum points or absolute minimum point with local curvature tending to zero, at least in pre-defined directions, as already demonstrated in [22].

Leroy et al. [15] have recently proposed a modification of Han et al. [1] and Colin et al. [23] approach, able to provide a continuous prediction of the induction/vulcanization/reversion sequence. The procedure has been then refined further by Milani et al. in [2], where a non trivial kinetic scheme with seven constants has been proposed, describing reversion by means of the distinct decomposition of single/double and multiple S–S bonds. Some other approaches roughly basing on the

same principles may be also found in [16–18]. However, in almost all the totality of the cases, the two major limitations previously described are not circumvented and the final success of the method is strongly dependent on the starting point adopted within the least squares routine adopted.

In the present paper, attention is focused on finding a procedure to determine kinetic constants without the utilization of both Runge-Kutta solvers and least squares optimization routines.

In particular, for the sake of simplicity, the general reaction scheme proposed by Han et al. [1] for vulcanized sulphur NR is assumed as initial base to interpret NR rheometer tests. No slight modifications are introduced, in order to make the results reproducible to any practitioner interested in the prediction of the kinetic behavior of NR cured with sulphur. Despite its limitations, Han et al. [1] model has the advantage to provide a closed form expression for the vulcanization degree, i.e. the utilization of a Runge-Kutta approach to solve a system of differential equations is not needed. However, three kinetic constants must be determined in the model by least-squares fitting on the experimental rheometer curves, thus the numerical complexity remains, with all the typical limitations linked to non-linear optimization (lack of convergence, multiple solutions, quasi optimality of some solutions far from the real one, etc.).

Here a different approach is proposed, that avoids the utilization of both Runge-Kutta routines to solve PDEs and least-squares procedures to fit experimental data.

The computational base adopted is represented by the kinetic scheme proposed by Han et al. [1]. Despite its rough approximations, it has the undoubtable advantage to provide a closed form expression for the vulcanization degree. In agreement with consolidated literature in the field, the rheometer test is assumed as the base to tune numerical kinetic constants.

After the normalization of the rheometer curves and the exclusion of induction period from calculations, the model requires the estimation of three kinetic constants, two of them describing incipient curing and stable crosslinks formations, the last reproducing reversion phenomenon.

As a matter of fact, see for instance Leroy et al. [15], kinetic constants are estimated by least-squares best fitting. However, such approach, whilst is undoubtable very straightforward at the same time proved to be rather cumbersome, sometimes fails to converge and/or provides suboptimal solutions, i.e. numerical rheometer curves very near to the experimental ones, but with associated kinetic constants totally wrong. In order to avoid such kind of difficulties, here a new and totally different procedure is proposed, which is intrinsically stable and is capable of providing both very good approximations of the experimental rheometer curves and reasonable estimates of kinetic constants, at a fraction of the time needed by least-squares fitting.

The procedure requires as input parameters only the degree of vulcanization at infinite (i.e. at the end of vulcanization), the instant where the maximum torque is reached and the initial rate of vulcanization. The condition that the numerical curve reaches a maximum at a given time translates mathematically into a non-linear equation in two of the kinetic constants. The implicit curve representing such condition is determined iteratively. Finally, the numerical initial vulcanization rate is tuned in such a way to globally minimize the absolute error between numerical and experimental curves.

Table 1 Rubber blend composition tested in rheometer experimentation of Fig. 1

Component	Parts (by weight)
Rubber gum	100
Carbon black	25
Oil	5
(ZnO / stearic acid) activator	6
Sulphur	3
Amine antioxidant	2

To estimate the fitting capabilities of the mathematical model proposed, five experimental rheometer curves at different temperatures on a same rubber blend are considered. Very good agreement with experimental data is observed.

The main novelty of the model stands therefore in the closed form determination of the kinetic constants representing the rates of the single reactions in the kinetic scheme adopted.

The evaluation of kinetic constants at three vulcanization temperatures, after proper check of the linearity in the Arrhenius space, allows performing numerical simulations at curing temperatures outside the range experimentally inspected, making the model predictive in all those cases where a wide experimental campaign is not possible.

2 Experimental rheometer curves used to benchmark the numerical model

Some experimental data referred to the isothermal curing of a NR blend with properties reported in Table 1 are at disposal from [2] and [15]. The blend was studied at five different temperatures, from 130 to 170 °C, with a temperature step equal to 10 °C. A Moving Die Rheometer MDR in dynamic mode (1 Hz) was used to collect the experimental curves.

The torque $S'(t)$ experimentally determined can be then used to estimate the vulcanization degree $\alpha_{exp}(t)$, using the following relationship proposed by Sun and Isayev [24]:

$$\alpha_{exp}(t) = \frac{S'(t) - S_{\min T}}{S_{\max T_0} - S_{\min T_0}} \tag{1}$$

where:

- $S_{\min T}$ is the S' minimum value at temperature T. Before reaching this minimum value, $\alpha_{\exp}$ is considered equal to zero.
- $S_{\min T0}$ and $S_{\max T0}$ are the minimum and maximum torque values at a curing temperature equal to T_0 low enough to allow neglecting reversion. In other words, the low temperature "reversion free" increase of mechanical properties during cure is taken as a reference, to estimate the influence of reversion at higher temperatures, which obviously results in a final degree of vulcanization lower than 100 %.

Figure 1a shows the typical torque–curing time curves obtained experimentally at the different vulcanization temperatures. As can be noted, the reversion phenomenon,

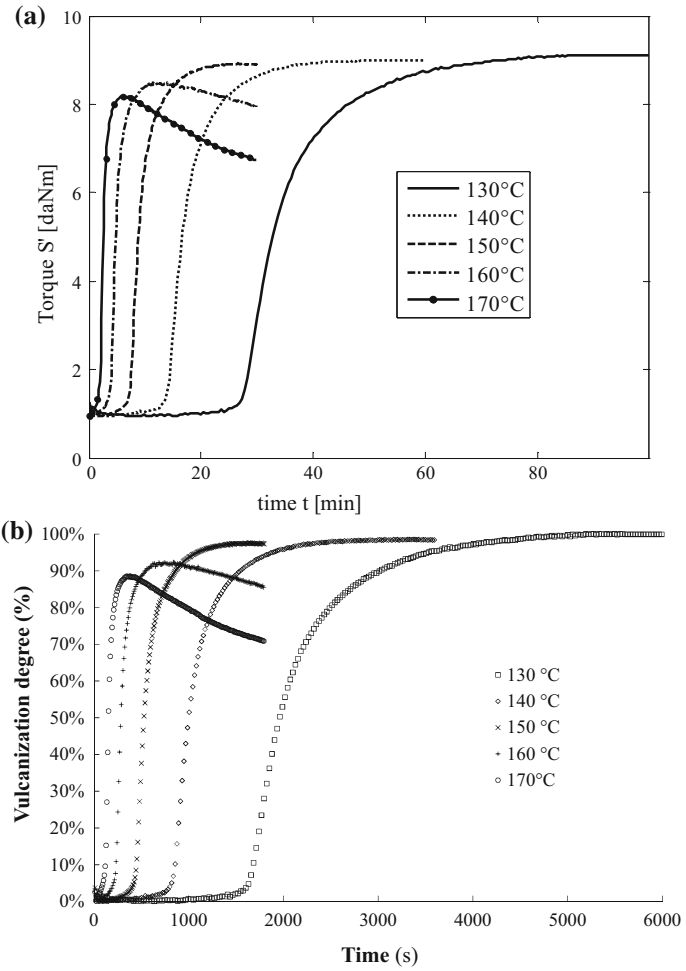

Fig. 1 **a** Experimental rheometer *curves* at temperatures from 130 to 170 °C (step 10 °C) **b** calculated vulcanization degree *curves* from Sun and Isayev [24] relationship (*note* induction, i.e. the *curve* before scorch point, is not excluded from computations)

which can be clearly observed at 160 and 170 °C, almost vanishes at 140 °C and at 130 °C, where the torque clearly reaches a horizontal plateau at the end of the experiments.

3 Han's model and iterative evaluation of kinetic constants

The basic reaction schemes assumed are classic and refer to existing literature in the field. Such schemes are known from the scientific literature, as mentioned above, see for instance [1,2,15,19,25].

Here for the sake of simplicity, the Han's model [1] is assumed, which will be briefly recalled in what follows.

As universally accepted, many reactions occur in series and parallel during NR curing with sulphur. After a viscous phase which characterizes the uncured rubber at high temperature and called "induction", the chain reactions are initiated by the formation of precursors, characterized by the kinetic constant K_1.

Then, curing proceeds through two pathways, with the formation of stable and unstable unmatured cured rubber. The distinction between stable and unstable curing stand in the presence of single or multiple sulphur bonds respectively. Multiple S–S bonds are intuitively less stable, and the evolution to matured cross-linked rubber is again distinct between the single S link between chains and the multiple one, statistically much less strong and leading to break with higher probability.

All the reactions considered occur with a kinetic velocity depending on the curing temperature, associated to each kinetic constant.

Let us assume that K_i is the i-th kinetic constant associated to one of the previously described phases, so that K_0 describes induction, K_1 and K_2 the formation of unmatured polymer, one stable and the other instable, and K_3 describes reversion.

Within such assumptions, we adopt for NR the kinetic scheme constituted by the chemical reactions summarized in the following set of equations:

$$\begin{aligned}
&[A_c] + [S] \xrightarrow{k_0} \left[A_1^*\right] \\
&\left[A_1^*\right] \xrightarrow{k_1} \left[R_1^*\right] \\
&\left[A_1^*\right] \xrightarrow{k_2} [R_1] \\
&[R_1] \xrightarrow{k_3} \left[R_1^D\right]
\end{aligned} \tag{2}$$

In Eq. (2), $[A_c]$ is a generic accelerator, $[S]$ is sulphur concentration, $\left[A_1^*\right]$ the sulphurating agent, $\left[R_1^*\right]$ the stable crosslinked chain (S–S single bonds), $[R_1]$ the unstable vulcanized polymer, $\left[R_1^D\right]$ the de-vulcanized polymer fraction (reversion). $K_{0,1,2,3}$ are kinetic reaction constants. Here it is worth emphasizing that $K_{0,1,2,3}$ are temperature dependent quantities, hence they rigorously should be indicated as $K_{0,1,2,3}(T)$, where T is the absolute temperature. In what follows, for the sake of simplicity, the temperature dependence will be left out.

The interaction between K_1 and K_2, from a chemical point of view, is associated with the formation of the activated complex and hence is linked to the activity and concentration of $\left[A_1^*\right]$. K_3 is reported by Han [1] to be responsible for reversion after the peak torque, as chemically confirmed by reactions in (2).

K_0 is the kinetic constant representing the induction period, that can be excluded from the computations assuming that the induction is evaluated by means of a first order Arrhenius equation.

According to the reaction scheme (2), excluding induction, the following differential equations may be written:

$$
\begin{aligned}
&\text{(a)} \quad \frac{d\left[A_1^*\right]}{dt} = -\left(K_1 + K_2\right)\left[A_1^*\right] \\
&\text{(b)} \quad \frac{d\left[R_1^*\right]}{dt} = K_1\left[A_1^*\right] \\
&\text{(c)} \quad \frac{d\left[R_1\right]}{dt} = K_2\left[A_1^*\right] - K_3\left[R_1\right]
\end{aligned} \tag{3}
$$

Equation (3)(a) may be trivially solved by separation of variables, as follows:

$$
\begin{aligned}
&\text{(a)} \quad \left[A_1^*\right] = \left[A_1^*\right]_0 e^{-(K_1+K_2)(t-t_i)} \\
&\text{(b)} \quad \frac{d\left[R_1^*\right]}{dt} = K_1\left[A_1^*\right]_0 e^{-(K_1+K_2)(t-t_i)} \\
&\text{(c)} \quad \frac{d\left[R_1\right]}{dt} = k_2\left[A_1^*\right]_0 e^{-(K_1+K_2)(t-t_i)} - K_3\left[R_1\right]
\end{aligned} \tag{4}
$$

Once $\left[A_1^*\right]$ is a known analytically function, $\left[A_1^*\right]$ can be substituted into Eqs. (b) and (c) in (4) to provide $\left[R_1^*\right]$ and $[R_1]$:

$$
\begin{aligned}
&\text{(a)} \quad \left[R_1^*\right] = \frac{K_1\left[A_1^*\right]_0}{K_1 + K_2}\left[1 - e^{-(K_1+K_2)(t-t_i)}\right] \\
&\text{(b)} \quad \frac{d\left[R_1\right]}{dt} + K_3\left[R_1\right] = K_2\left[A_1^*\right]_0 e^{-(K_1+K_2)(t-t_i)}
\end{aligned} \tag{5}
$$

(5)(b) is a non homogeneous first order linear differential equation, which admits the following solution composed by a general and a particular root:

$$
\left[R_1\right] = \frac{K_2}{K_1 + K_2 - K_3}\left[A_1^*\right]_0\left[e^{-K_3(t-t_i)} - e^{-(K_1+K_z)(t-t_i)}\right] \tag{6}
$$

The final concentration of vulcanized rubber is thus $\left[R_1^*\right] + [R_1]$:

$$
\begin{aligned}
\left[R_1\right] + \left[R_1^*\right] = &\frac{K_1\left[A_1^*\right]_0}{K_1 + K_2}\left[1 - e^{-(K_1+K_2)(t-t_i)}\right] \\
&+ \frac{K_2}{K_1 + K_2 - K_3}\left[A_1^*\right]_0\left[e^{-K_3(t-t_i)} - e^{-(K_1+K_2)(t-t_i)}\right]
\end{aligned} \tag{7}
$$

(7) can be normalized with respect to $[S]_0$ as follows:

$$
\begin{aligned}
\alpha = \frac{\left[R_1\right] + \left[R_1^*\right]}{[S]_0} = &\frac{K_1}{K_1 + K_2}\left[1 - e^{-(K_1+K_2)(t-t_i)}\right] \\
&+ \frac{K_2}{K_1 + K_2 - K_3}\left[e^{-K_3(t-t_i)} - e^{-(K_1+K_2)(t-t_i)}\right]
\end{aligned} \tag{8}
$$

Note that first derivative of (8) is:

$$\frac{d\alpha}{dt} = K_1 e^{-(K_1+K_2)(t-t_i)} + \frac{K_2}{K_1 + a_2 - k_3}\left[-K_3 e^{-K_3(t-t_i)} + (K_1 + K_2)\, e^{-(K_1+K_2)(t-t_i)}\right] \quad (9)$$

Normally constants $K_{1,2,3}$ are evaluated by least-squares best fitting [15]. A direct evaluation that needs very trivial numerical routines is proposed herein for the first time.

In Eq. (12), we make the hypothesis that:

$$\lim_{t\to+\infty} \alpha = \alpha_R = \frac{K_1}{K_1 + K_2} \quad (10)$$

Equation (10) provides a relation between constants K_1 and K_2. In particular, K_2 is K_1 dependent as follows:

$$K_2 = \frac{1-\alpha_R}{\alpha_R} K_1 \quad (11)$$

Assuming that the maximum of the normalized rheometer curve is reached at $t = t_M$ we obtain the relation:

$$\left.\frac{d\alpha}{dt}\right|_{t=t_M} = \frac{K_2}{K_1 + K_2 - K_3}\left[-K_3 e^{-K_3(t_M-t_i)} + (K_1 + K_2)\, e^{-(K_1+K_2)(t_M-t_i)}\right] = 0 \quad (12)$$

It is interesting to notice that Eq. (12) can be re-written as follows:

$$K_3 = \frac{(K_1 + K_2)^2\, e^{-(K_1+K_2)(t_M-t_i)}}{K_1 e^{-(K_1+K_2)(t_M-t_i)} + K_2 e^{-K_3(t_M-t_i)}} \quad (13)$$

And using Eq. (11):

$$K_3 = \frac{\frac{K_1^2}{\alpha_R^2} e^{-\frac{K_1(t_M-t_i)}{\alpha_R}}}{K_1 e^{-\frac{K_1(t_M-t_i)}{\alpha_R}} + \frac{1-\alpha_R}{\alpha_R} K_1 e^{-K_3(t_M-t_i)}} \quad (14)$$

Equation (14) is particularly interesting because it allows to iteratively estimate K_3 at a fixed value of K_1. The algorithm used is explained in the pseudo-code of Table 2.

A typical $K_3 - K_1$ interaction curve obtained for a practical case is depicted in Fig. 2. The authors experienced some common features at different temperatures and differ compound concentrations, as for instance:

1) The curve is regular and monothonic. It is defined only for K_1 greater than the point of intersection between the curve and the straight line $K_1 + K_2 - K_3 = \frac{K_1}{\alpha_R} - K_3$. Let's indicate with $K_1^{\min}$ such minimum point.

Table 2 Pseudo code for the determination of K_3

Step 1: Fix a value for $K_1 = \bar{K}_1$

Step 2A: Fix an initial value for $K_3 = K_3^{(i)} = 0$

Step 2B: Find a new value of $K_3 = K_3^{(n)} = \dfrac{\frac{K_1^2}{\alpha_R^2} e^{-\frac{K_1(t_M - t_i)}{\alpha_R}}}{K_1 e^{-\frac{K_1(t_M - t_i)}{\alpha_R}} + \frac{1-\alpha_R}{\alpha_R} K_1 e^{-K_3^{(i)}(t_M - t_i)}}$

IF $|K_3^{(n)} - K_3^{(i)}|$ <TOL (TOL desired tolerance) $K_3^{(f)} = K_3^{(n)}$ END

ELSE $K_3^{(i)} = K_3^{(n)}$

REPEAT Step 2B

REPEAT Step 1

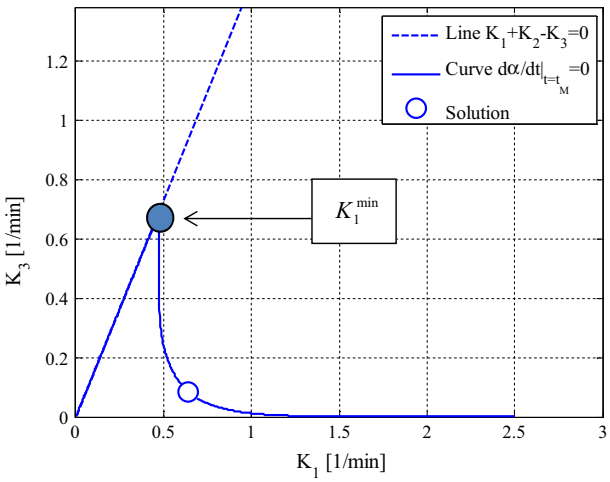

Fig. 2 Typical $K_3 - K_1$ interaction *curve* found numerically with the algorithm reported in Table 2

Table 3 Pseudo code for the determination of K_1 and K_3

Step 1: Determine graphically $K_1^{\min}$ and fix a reasonable value for $K_1^{\max}$

Step 2A: FOR $K_1^{\min} \le K_1 \le K_1^{\max}$, $1 \le i \le N_{sud}$ N_{sud}: number of subdivisions $K_1^i = K_1^{\min} + \frac{(i-1)}{N_{sud}} \left(K_1^{\max} - K_1^{\min}\right)$

Step 2B: With K_1^i, find K_3 on the curve of Fig. 2. Find K_2 as $K_2 = \frac{1-\alpha_R}{\alpha_R} K_1$

Step 2C: With K_1, K_2 and K_3 evaluate the fitting property of the numerical curve and compare it with experimental data, assuming as fitting parameter the cumulative absolute error.

REPEAT Step 2A for all K_1^is

SELECT the curve exhibiting lower cumulated error.

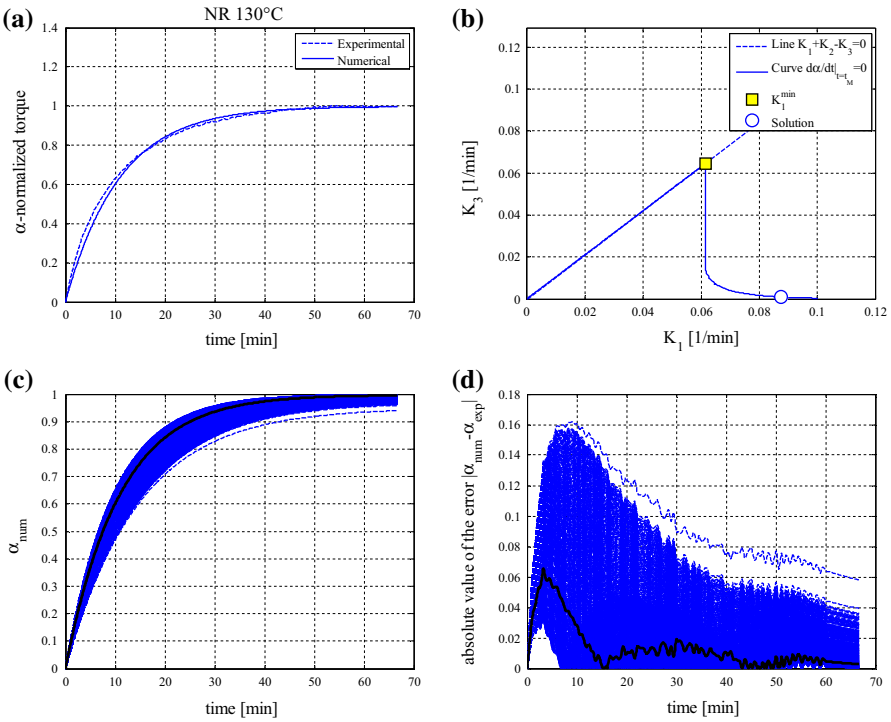

Fig. 3 130 °C. **a** comparison between experimental (after normalization) and numerical rheometer *curves*. **b** Evaluation of K_3 by means of the iterative algorithm of Table 2 and implicit function of eq. (13). **c** Family of numerical rheometer *curves* varying K_1 from $K_1^{\min}$ to $K_1^{\max} = 3K_1^{\min}$ (*black thick curve* represents the optimal one). **d** Representation of the absolute value of the total error for the family of rheometer *curves* represented in subfigure **c** (*black thick curve* represents the optimal solution)

2) The drop of the curve (first derivative) is particularly marked near $K_1^{\min}$. Conversely, very small values of K_3 are found with a corresponding K_1 which is 2–3 times $K_1^{\min}$.

We also assume that at scorch the rate of vulcanization is α_0', i.e. from Eq. (9):

$$\left.\frac{d\alpha}{dt}\right|_{t=t_i} = \alpha_0' = K_1 + K_2 = \frac{K_1}{\alpha_R} \tag{15}$$

The strategy adopted in this second phase to define constant K_1 at the solution point is the following:

1) We assume a trial value of the first derivative at the scorch point ($\left.\frac{d\alpha}{dt}\right|_{t=t_i}$). According to Eq. (15), such condition reduces to select a trial value for K_1.
2) With such trial value, through Eq. (11) and Fig. 2, K_2 and K_3 are obtained respectively, i.e. a numerical normalized rheometer curve can be built.
3) K_1 that minimizes the absolute error of the numerical curve when compared with the normalized experimental one is assumed as the solution of the optimization problem.

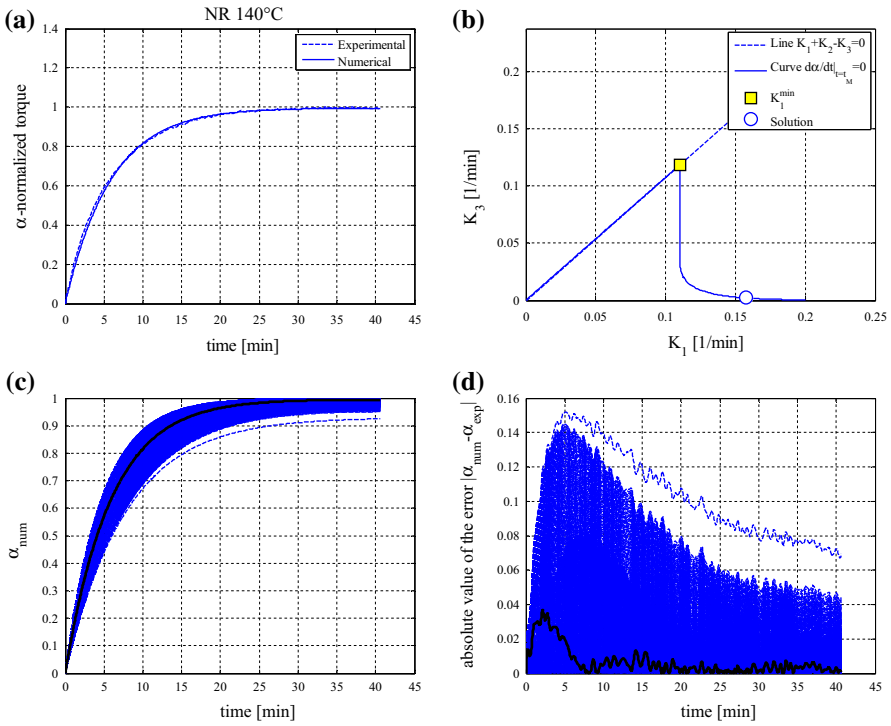

Fig. 4 140 °C. **a** Comparison between experimental (after normalization) and numerical rheometer *curves*. **b** Evaluation of K_3 by means of the iterative algorithm of Table 2 and implicit function of Eq. (13). **c** Family of numerical rheometer *curves* varying K_1 from $K_1^{\min}$ to $K_1^{\max} = 3K_1^{\min}$ (*black thick curve* represents the optimal one). **d** Representation of the absolute value of the total error for the family of rheometer *curves* represented in subfigure **c** (*black thick curve* represents the optimal solution)

4) A reasonable interval for the research of the optimal K_1 variable is *a-priori* assumed for the sake of simplicity. The lower bound is obviously constituted by $K_1^{\min}$. However, according to Eq. (15), $\frac{d\alpha}{dt}\Big|_{t=t_i}$ may, at least in principle, exhibit infinite value at the scorch point, meaning that K_1 does not have an upper bound. This notwithstanding, as already pointed out for K_1 exceeding 2-3 times $K_1^{\min}$, K_3 in practice vanishes, thus providing rheometer curves rarely in agreement with experimental evidences.

For the sake of clearness, the pseudo code utilized in the paper to estimate K_1 and K_3 is represented in Table 3. Here the search domain is subdivided in equally stepped intervals and each interval extreme represented a sampled point (couple of K_1 and K_3 values). However, it is worth noting that more sophisticated and effective procedures may be easily implemented, including a Newton bisection method [26] or meta-heuristic approaches like Genetic Algorithms [27].

The need to implement more complex numerical approaches is however here not paramount, because the computational effort needed for the optimization remains rather low even when the algorithm of Table 3 is adopted.

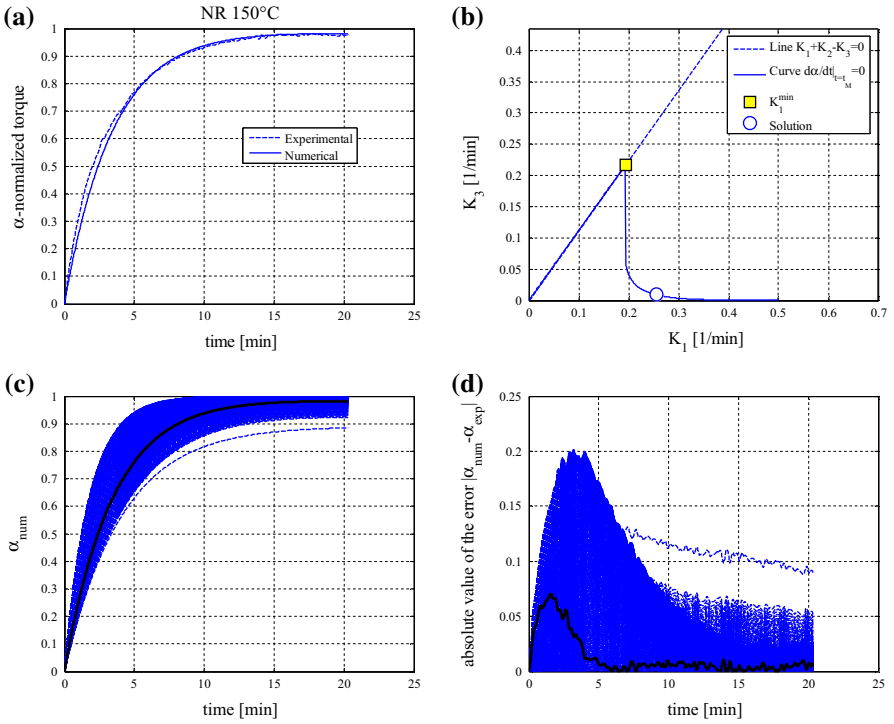

Fig. 5 150 °C. **a** Comparison between experimental (after normalization) and numerical rheometer *curves*. **b** Evaluation of K_3 by means of the iterative algorithm of Table 2 and implicit function of Eq. (13). **c** Family of numerical rheometer *curves* varying K_1 from $K_1^{\min}$ to $K_1^{\max} = 3K_1^{\min}$ (*black thick curve* represents the optimal one). **d** Representation of the absolute value of the total error for the family of rheometer *curves* represented in subfigure **c** (*black thick curve* represents the optimal solution)

4 Numerical simulations

In this Section, the reliability of the iterative approach proposed is tested on the set of experimental rheometer curves discussed in Sect. 2. Attention is focused exclusively on the capabilities of the numerical approach to fit experimental evidences.

As already discussed, Fig. 1a shows the typical torque vs. time curves obtained at the different cure temperatures. Reversion is clearly observed at 160 and 170 °C, whereas it becomes negligible at 140 °C, and at 130 °C

Figure 1b is used to tune numerical kinetic constants. It represents the experimental vulcanization degree $\alpha_{\exp}(t)$ derived from average $S'(t)$ torque by means of the relation proposed by Sun and Isayev [24]. As the difference between ($S'_{\max}$ 130 °C − $S'_{\min}$ 130 °C) and ($S'_{\max}$ 140 °C − $S'_{\min}$ 140 °C) is lower than 2 %, the value at 130 °C is used for the calculation of the degree of vulcanization according to [24].

In addition, the induction time is disregarded and Fig. 1b curves are simply shifted to the origin. As already pointed out, indeed, rubber behavior at the beginning is viscous and any kinetic model of vulcanization would fail to fit experimental evidences there,

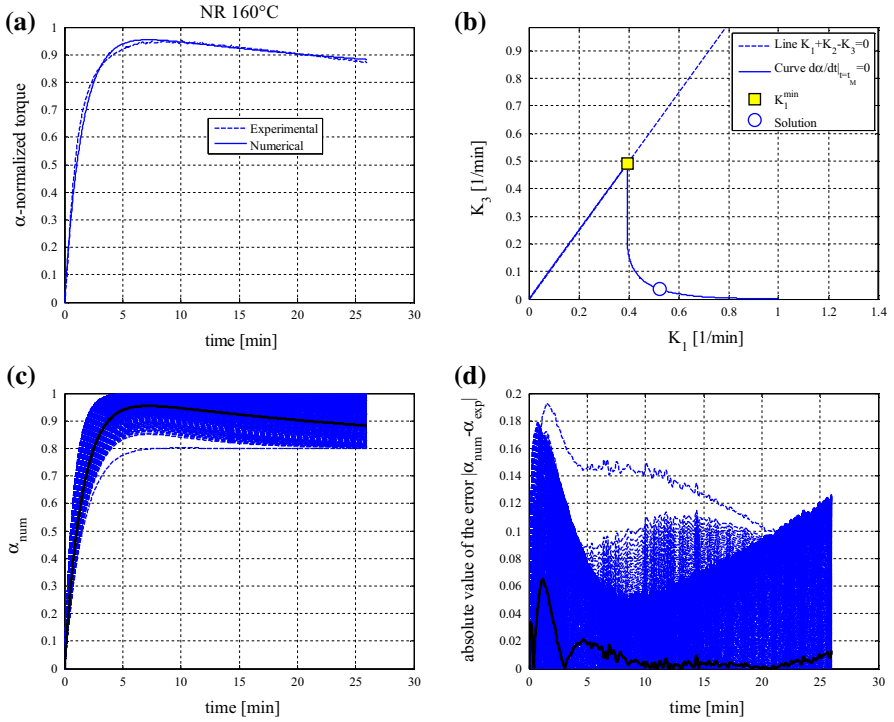

Fig. 6 160 °C. **a** Comparison between experimental (after normalization) and numerical rheometer *curves*. **b** Evaluation of K_3 by means of the iterative algorithm of Table 2 and implicit function of Eq. (13). **c** Family of numerical rheometer *curves* varying K_1 from $K_1^{\min}$ to $K_1^{\max} = 3K_1^{\min}$ (*black thick curve* represents the optimal one). **d** Representation of the absolute value of the total error for the family of rheometer *curves* represented in subfigure **c** (*black thick curve* represents the optimal solution)

simply because the approach chosen does not represent the physical phenomenon occurring before the begin of vulcanization.

The results obtained by means of the numerical approach proposed in the paper are represented from Figs. 3, 4, 5, 6 and 7, starting from normalized rheometer curves at 130 °C (Fig. 3) and ending with curves at 170 °C (Fig. 7).

For each vulcanization temperature (and hence for each figure), the following plots are represented: in subfigures-a a comparison between experimental (after normalization) and numerical rheometer curves is depicted; in subfigures-b the evaluation of K_3 by means of the iterative algorithm of Table 2 and implicit function of Eq. (13) is provided; in subfigures-c the family of numerical rheometer curves varying K_1 from $K_1^{\min}$ to $K_1^{\max} = \rho K_1^{\min}$ with ρ coefficient depending case by case (black thick curve represents the optimal one) is depicted; finally in subfigures-d a representation of the absolute value of the total error for the family of rheometer curves represented in subfigure-c (black thick curve represents again the optimal solution) is provided.

From a detailed analysis of simulations results, it can be seen that the numerical procedure proposed fits extremely well experimental results, with an almost perfect agreement for all the temperatures inspected and even in the de-vulcanization range,

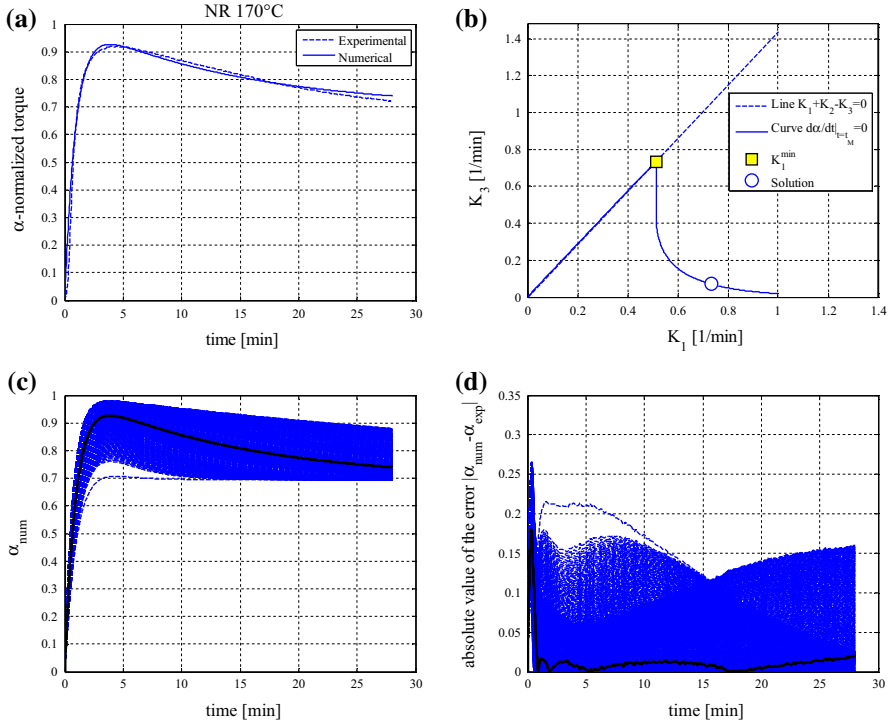

Fig. 7 170 °C. **a** Comparison between experimental (after normalization) and numerical rheometer *curves*. **b** Evaluation of K_3 by means of the iterative algorithm of Table 2 and implicit function of Eq. (13). **c** Family of numerical rheometer *curves* varying K_1 from $K_1^{\min}$ to $K_1^{\max} = 3K_1^{\min}$ (*black thick curve* represents the optimal one). **d** Representation of the absolute value of the total error for the family of rheometer *curves* represented in subfigure **c** (*black thick curve* represents the optimal solution)

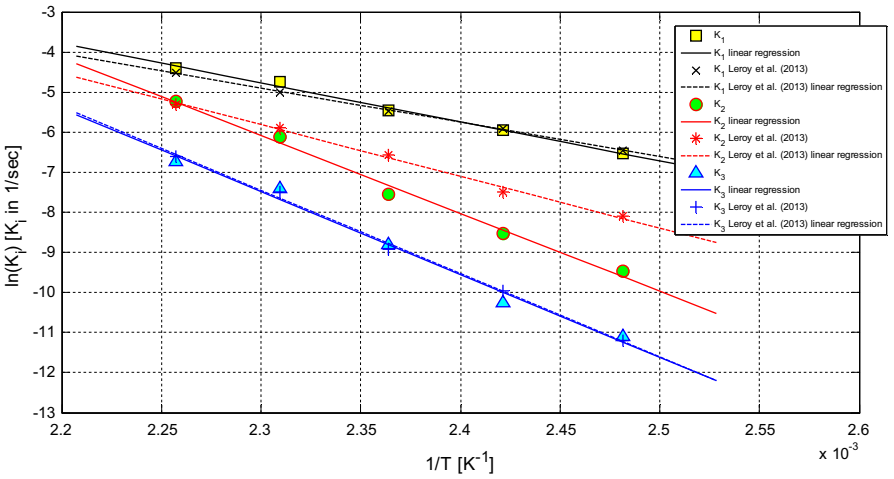

Fig. 8 Overall comparison among K_i constants for the cases analyzed in the Arrhenius space

when present. Small differences may be appreciated after a proper zoom of the curves at the very beginning or near the initiation of reversion in some few cases, however much less evident than deviations obtained applying simplified models available in existing literature.

The numerical rheometer curve is very near to the experimental one in absence of reversion, i.e. at low temperature (130 and 140 °C), but appears extremely satisfactory even in presence of visible reversion (170 °C).

The total error estimation for the optimal solution appears almost constant increasing the vulcanization temperature, compare for instance Figs. 3 and 7.

5 Conclusions

A novel closed form approach to determine kinetic constants describing incipient curing, matured crosslinking and reversion in NR vulcanized with sulphur has been presented in the paper.

Starting from a previously presented vulcanization model that allows deriving a simple closed-form expression for the curing degree, the determination of the kinetic constants is performed in closed form, without the need to utilize classic least squares approaches. The model has been benchmarked on a NR blend vulcanized at five different temperatures. From simulations results, it was found that the kinetic constants follow reasonably well an Arrhenius law, see Fig. 8, which represents one of the most useful relationships in chemical kinetics, when an extrapolation of the behavior is needed outside the experimentally tested temperature range. In Fig. 8 there is also a comparison with K_i numerical results found by Leroy et al. in [15]. In [15], Han's model is used and K_i are evaluated by standard least-squares fitting. As can be noted, the agreement for what concerns K_1 and K_3 is almost perfect, whereas some discrepancies are experienced for K_2. This is not surprising, because the closed form solution proposed requires an evaluation of K_2 through the definition of the reversion percentage, see Eq. (11). With very little reversion or in absence of reversion, Eq. (11) is clearly affected by high scatter. To confirm such deduction, it can be observed from Fig. 8 that the evaluated values of K_2 for temperatures equal to 170 and 160 °C (i.e. where reversion is clearly visible) are almost superimposable to those found by Leroy et al. in [15].

References

1. I.S. Han, C.B. Chung, S.J. Kang, S.J. Kim, H.C. Chung, Polymer (Korea) **22**, 223–230 (1998)
2. G. Milani, E. Leroy, F. Milani, R. Deterre, Polym. Test. **32**, 1052–1063 (2013)
3. ASTM D2084–81 or ASTM D5289. ASTM Standard D5289. Oscillating disc and rotorless curometer tests Standard test method for vulcanization rubber and thermoplastic elastomers. Annual Book 2002
4. Y. Tanaka, Rubber Chem. Technol. **64**, 325 (1991)
5. G. Wolfman, Hasenhidl, S. Wolf, Kautschuk Gummi Kunststoffe **44**(2), 118 (1991)
6. A.Y. Coran, *Science and Technology of Rubber* (Academic Press, New York, 1978). Chapter 7
7. L. Pualing, *The Nature of the Chemical Bond* (Cornell University Press, Ithaca, 1959)
8. K.D.O. Jackson, M.J.R. Loadman, C.H. Jones, G. Ellis, Spectrochim. Acta **46**(2A), 217 (1990)
9. G. Ellis, P.J. Hendra, M.J.R. Loadman, Kautschuk Gummi Kunststoffe **43**(2), 118 (1990)
10. D.J.P. Harrison, W.R. Yates, J. Macromol. Sci. C **25**, 481 (1985)

11. A.M. Zaper, J.L. Koenig, Rubber Chem. Technol. **60**, 252 (1987)
12. R. Orza, P.C.M.M. Magusin, V.M. Litvinov, M. van Duin, M.A.J. Michels, Macromolecules **42**, 8914–8924 (2009)
13. H.G. Dikland, M. van Duin, Crosslinking of EPDM and polydiene rubbers studied by optical spectroscopy, in *Spectroscopy of Rubbers and Rubbery Materials*, ed. by V.M. Litvinov, P.P. De (Rapra Technology Ltd., Shawbury, 2002), p. 207
14. T. Kemperman, Kautschuk Gummi Kunststoffe **40**, 820 (1987)
15. E. Leroy, Souid, R. Deterre, Polym. Test. **32**, 575–582 (2013)
16. G. Milani, F. Milani, J. Appl. Polym. Sci. **119**, 419–437 (2011)
17. G. Milani, F. Milani, J. Math. Chem. **52**(2), 464–488 (2014)
18. G. Milani, F. Milani, Polym. Test. **33**, 1–15 (2014)
19. R. Ding, I. Leonov, J. Appl. Polym. Sci. **61**, 455 (1996)
20. R. Ding, I. Leonov, A.Y. Coran, Rubber Chem. Technol. **69**, 81 (1996)
21. M.R. Kamal, S. Sourour, Polym. Eng. Sci. **13**, 59–64 (1973)
22. G. Milani, J. Math. Chem. **51**, 465–497 (2013)
23. X. Colin, L. Audouin, J. Verdu, Polym. Degrad. Stab. **92**(5), 906–914 (2007)
24. X. Sun, A.I. Isayev, Rubber Chem. Technol. **82**(2), 149–169 (2009)
25. R.P. Quirk, Prog. Rubber Plast. Technol. **4**(1), 31 (1988)
26. G. Milani, F. Milani, J. Appl. Polym. Sci. **115**, 1995–2012 (2010)
27. G. Milani, F. Milani, Comput. Chem. Eng. **32**, 3198–3212 (2008)